Wurtzite InP formation during swift Xe-ion irradiation

P. I. Gaiduk,* F. F. Komarov, and V. S. Tishkov
Belarusian State University, Kurchatova 7, 220064 Minsk, Belarus

W. Wesch and E. Wendler
Friedrich-Schiller-Universitaet Jena, Institut fuer Festkoerperphysik, Max-Wien-Platz 1, D-07743 Jena, Germany

(Received 6 May 1999; revised manuscript received 28 October 1999)

Ion beam-induced amorphization and crystallization in InP implanted at room temperature with swift (250 and 340 MeV) Xe^+ ions to doses of 5×10^{13} and $1\times10^{14}\,cm^{-2}$, respectively, are investigated by transmission electron microscopy. For ion fluences above $5\times10^{13}\,cm^{-2}$, amorphization is registered in the near-surface region as well as around the mean ion range. The amorphous layers produced due to electronic energy deposition in the near-surface region are found to have different short-range atomic structure as compared to those produced in the depth region of nuclear energy deposition. In the case of the highest ion fluence ($1\times10^{14}\,cm^{-2}$) a partial crystallization of the amorphous surface layer to polycrystalline InP is observed. The process of the crystallization passes a stage of wurtzite InP phase formation.

I. INTRODUCTION

Swift heavy-ion implantation is known to result in a number of effects (latent tracks, high pressure phases, fullerenes, etc.) in solids due to dissipation of the high electronic excitation arising from inelastic collisions.[1–3] Recently, we have reported on the formation of latent tracks and continuous amorphous layers in InP irradiated with 250 MeV Xe^+ ions.[4] After the implantation to a dose of $7\times10^{12}\,Xe^+/cm^2$ latent tracks are registered in a near-surface region of InP where the ions lose their energy preferentially into the electronic subsystem. The tracks overlap producing a continuous amorphous layer in the surface region when the dose is increased up to $5\times10^{13}\,cm^{-2}$. For this ion fluence a second amorphous layer is registered at the depth of the mean projected range (R_p), where the ions lose their energy preferentially by nuclear collisions. Generally, one can expect that different mechanisms of amorphization may result in a different atomic structure of the amorphous layer. However, to our knowledge, no results on this topic are published up to now.

The present paper deals with the results of a comparative investigation of both near-surface and near R_p amorphous layers produced by swift Xe^+ ions in InP. The crystallization of these layers is also studied.

II. EXPERIMENT

Xe ions with energies of 250 and 340 MeV were implanted into ⟨100⟩-cut single crystalline InP wafers at room temperature. The ion fluence was varied between $5\times10^{13}\,cm^{-2}$ and $1\times10^{14}\,cm^{-2}$. To prevent sample heating during the irradiation the flux was kept below $1.3\times10^{10}\,Xe\,cm^{-2}\,s^{-1}$. Additionally, the samples were mounted to the sample holder with a silver paste in order to provide a good thermal conductivity between them. The implanted layers were investigated using cross-section transmission electron microscopy (XTEM). The conventional TEM investigations were performed with an electron microscope EM-125 operating at 100 keV. For observations in high-resolution TEM mode (HRTEM) the device Philips CM20 operating at 200 keV was applied. The control of the sample stoichiometry by x-ray energy dispersive spectrometry was carried out using a Philips CM20/EDAX PV9800 instrument. The TEM specimen were thinned down to electron transparency using an ion beam sputtering technique. In order to prevent sample heating and artefacts of etching (selective sputtering, In segregation on the surface) ion beam milling was performed at liquid nitrogen temperature, and the angle between the ion beam and the sample surface was lower than 5°–7°. The interplane distances for both sphalerite (B3-type) and hexagonal (wurtzite) InP (B4-type) were calculated assuming that InP of wurtzite structure consists of tetrahedrons with the same geometrical size as those of the B3-type, but with an ABAB...AB stacking sequence.[5]

III. RESULTS AND DISCUSSION

In accordance with our previous work[4] it is found that InP samples implanted with $5\times10^{13}\,Xe^+\,cm^{-2}$ contain two continuous amorphous layers (AL) separated by a single crystalline InP region with extended defects of a different type. From XTEM pictures received over the whole implanted depth it was deduced that the first AL is located in the near-surface region expanding into depths down to 12 and 15 μm for 250 and 340 MeV irradiations, respectively. The simulation of the depth distributions of electronic and nuclear energy deposition per ion and unit length using the TRIM 95 code shows that in this depth region electronic processes dominate (not shown), and that nuclear interactions can be neglected. The second AL with a thickness of about 3–5 μm is formed at the depth of about 21 and 26 μm (corresponding to the projected range R_p) for the two energies used, i.e., it is located in the region of high nuclear interaction. The AL thicknesses mentioned above are found to be large enough to study the structure of the samples in a cross-section geometry by using both bright- (dark-) field imaging and microdiffraction techniques, assuming a homogeneous structural quality within the areas of investigation (typically less than 2

0163-1829/2000/61(23)/15785(4)/$15.00 PRB 61 ©2000 The American Physical Society

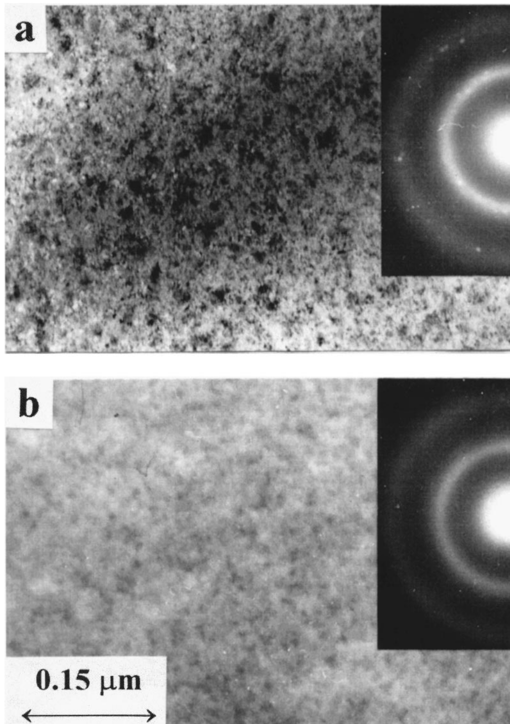

FIG. 1. Bright-field TEM images of the structure of near-surface (a) and near-R_p layers (b) of InP implanted with Xe^+ (250 MeV, $5\times10^{13}\,cm^{-2}$). The insets display the corresponding TED patterns.

μm wide). The damage in the near-surface and in the buried damage band was studied on samples thinned by cross-sectional preparation over the whole depth and in one step. Therefore a possible different action of sample preparation (irradiation conditions, sample heating, artefacts of etching, etc.) on the structural quality of the defect bands can be excluded. Moreover, to exclude a possible variation of the damage structure with the depth, the TEM study of the near-surface layer of each sample was performed at about 5 μm, and that of the buried layer at the depth of R_p. A visible stoichiometry decomposition of the layers (e.g., due to selective evaporation during swift Xe irradiation) was not registered by x-ray energy dispersive spectrometry.

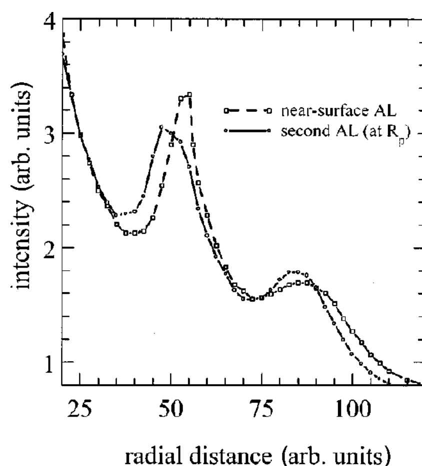

FIG. 2. Angular distributions of coherently scattered electrons obtained from the TED investigations of surface (a) and near-R_p (b) amorphous layers.

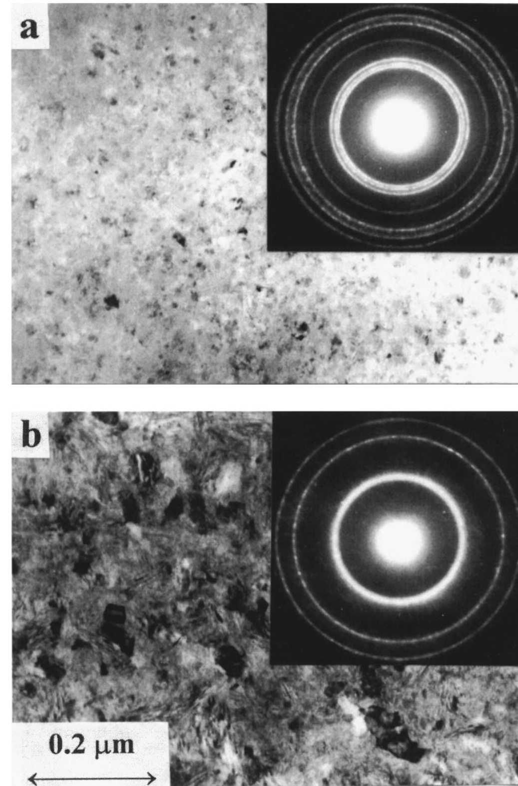

FIG. 3. Bright-field TEM images of the structure and corresponding TED patterns, obtained from the near-surface layer after beam-induced crystallization. (a) First stage of crystallization: the formation of fine-grain polycrystalline InP of the wurtzite modification after irradiation with $8\times10^{13}\,Xe\,cm^{-2}$. (b) Second stage of crystallization: the formation of polycrystalline InP of sphalerite modification after irradiation with $1\times10^{14}\,Xe\,cm^{-2}$.

The results of the TEM investigations have revealed differences in the structure of the two amorphous layers mentioned above. Typical bright-field TEM images of the structure and corresponding diffraction (TED) patterns of the two layers are shown in Fig. 1. It can be seen from the pictures that the contrast of the TEM image is sufficiently homogeneous in the near-R_p-AL [Fig. 1(b)], but has small-sized inhomogeneities in the surface AL [Fig. 1(a)]. Both diffraction patterns contain diffuse rings due to the amorphous state of InP; in addition, diffraction spots from crystalline particles of InP are visible in the case of the surface AL [TED pattern in Fig. 1(a)]. In the latter case, a dark-field TEM image obtained in ⟨220⟩ InP spots (not shown here) has proved that the nonhomogeneous contrast in Fig. 1(a) is due to crystalline particles embedded in the amorphous layer.

Figure 2 illustrates a comparison of the angular distributions of the intensity of electrons coherently scattered within the two disturbed layers. The distributions are compiled by radial scanning of the original TED patterns obtained from the near-surface and near-R_p amorphous layers of the same sample [see inset in Figs. 1(a) and 1(b)]. There are two strong differences in the electron intensity distributions of the two first diffraction maxima. First, the diffraction peaks obtained from the near-surface AL are located at larger radial distances from the center as compared to those from the near-R_p AL. And second, the half-widths of the diffraction peaks are different: the first peak is found to be more narrow

TABLE I. The interplane distances extracted from the electron diffraction patterns similar to those shown in Fig. 3(a)—(d_{e1}) and in Fig. 3(b)—(d_{e2}) in comparison with the calculated interplane distances of sphalerite—(d_s) and hexagonal (wurtzite)—(d_w) modification of InP.

hkl	d_{e1}	d_w	*hkl*	d_{e2}	d_s
100	3.57	3.578	-	-	-
002	3.38	3.374	111	3.39	3.391
101	3.16	3.161	200	2.94	2.937
102	2.46	2.455	-	-	-
110	2.06	2.066	220	2.08	2.076
103	1.91	1.904	-	-	-
200	1.78	1.789	-	-	-
112	1.76	1.762	311	1.76	1.771
201	1.73	1.729	222	1.69	1.695
202	1.58	1.581	400	1.46	1.468
203	1.40	1.400	-	-	-
210	1.34	1.353	331	1.35	1.347
211	1.32	1.326	420	1.30	1.313
212	1.26	1.255	-	-	-
300	1.19	1.193	-	-	-
213	1.16	1.159	422	1.21	1.199
006	1.12	1.125	511	1.12	1.130
205	1.08	1.077	-	-	-
220	1.03	1.033	440	1.03	1.038

in the case of the near surface compared to that of the near-R_p AL, for the second peak the behavior is opposite. These TED results directly indicate the strong differences in the atomic short-range order in the two amorphous layers.[6,7] Furthermore, comparative TED investigations of the near-R_p amorphous layers produced by the fast Xe ions and amorphous layers created with conventional ion energies (e.g., 100 keV Xe^+) have revealed very similar angular distributions of the coherently scattered electrons (not shown here).

Elevating the irradiation fluence up to $10^{14}\,cm^{-2}$ results in an increase of the thickness of both the surface and the near-R_p amorphous layers reflecting the accumulation of damage in the layers. However, as a very interesting consequence of the increasing ion dose a transformation of InP from the amorphous to the polycrystalline state was registered in the surface region. This recrystallization process starts from the surface, extends to the depth, and passes two main stages that result in a qualitatively different structure of the final polycrystalline phase [Figs. 3(a) and 3(b)]. At the first stage the amorphous InP is transformed into a fine-grain polycrystalline state [Fig. 3(a)]. This occurs for ion fluences of about $8\times10^{13}\,cm^{-2}$. The most surprising feature of this structure is that, according to the TED investigations, the fine-grain polycrystalline InP has a hexagonal (wurtzite) structure. This is proven by the microdiffraction pattern inserted in Fig. 3(a) and, respectively, by Table I and Fig. 4(a). The latter figure displays an angular distribution of the intensity of coherently scattered electrons in comparison with a theoretical x-ray-diffraction spectrum, calculated for the wurtzite modification of InP. The experimental curve was obtained by radial scanning of the original TED pattern obtained from the near-surface layer [inset in Fig. 3(a)]. A good correlation of both

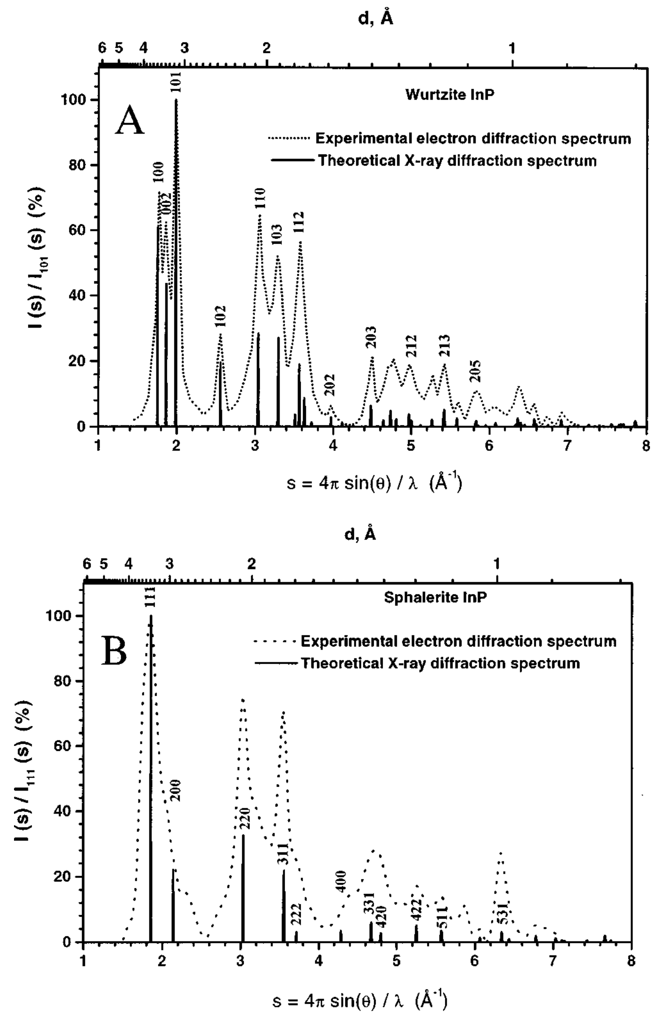

FIG. 4. Normalized intensity of coherently scattered electrons as a function of both extent in reciprocal space (s) and interplane distance (d) for wurtzite (A) and sphalerite (B) InP. The experimental curves are obtained by scanning of the original TED patterns shown as insets in Figs. 3(a) and 3(b) accordingly. The corresponding theoretical x-ray-diffraction spectra are shown.

theoretical and experimental data is to be seen from the figure.

The wurtzite modification of InP is found to be unstable. A transition from the wurtzite to the ordinary (sphalerite) structure occurs at the second stage of recrystallization as a result of both increasing the ion fluence up to $10^{14}\,cm^{-2}$ and (or) intensive electron beam irradiation in the TEM chamber during the investigation. The bright-field image of the final structure and the corresponding TED pattern are shown in Fig. 3(b). These pictures clearly show a polycrystalline structure with an average grain size of about 0.1–0.3 μm; in addition, the angular distribution of the intensity of coherently scattered electrons extracted from the original TED pattern [Fig. 4(b)] is found to be very close to InP of the sphalerite modification. Note again a good correlation between theoretical (calculated for sphalerite InP) and experimental data in Fig. 4(b) and Table I. Such a transition of amorphous to wurtzite and then to sphalerite structure was also found under a high-intensity electron beam (more than about 10 $\mu A/\mu m^2$) during the TEM investigation of the surface AL. Contrary, no indication of a recrystallization effect

was found in the near-R_p amorphous layer at the implantation fluences used and during high intensity electron-beam irradiation in the TEM chamber.

The hexagonal (wurtzite) phase has previously also been observed in silicon after mechanical deformation by indentation at high temperature (500–600 °C).[8,9] For pressures up to 50 GPa the silicon structure transforms from a cubic diamond to a β-Sn-like tetragonal one, and then to a hexagonal one (simple and close packed).[10] Recently, the formation of the wurtzite phase of silicon has been registered in a number of studies of high-dose, high-intensity, and high-temperature ion implantation.[9,11,12] This phase is found to be metastable with respect to the diamond cubic structure, but it is stabilized by the presence of internal stresses.[10,11] At very high implantation temperatures (>700 °C) the wurtzite phase cannot be formed due to easy motion of dislocations with the relief of the strain.[11]

Similarly, it is found[13] that under indentation in a diamond cell, InP transforms from the cubic, zinc-blende (sphalerite) phase to the cubic, rocksalt structure at ~10.8 GPa, to the β-Sn-like tetragonal phase at ~18.9 GPa; however, no indications of wurtzite phase formation were reported. The latter, probably, is due to the low value of the pressure used in Ref. 13. This conclusion is supported by the results on the structure transformation in Si and Ge which revealed a phase transformation from the β-Sn-like tetragonal to the wurtzite structure but under considerably higher pressures of indentation.[10] No data on implantation-induced phase changes in InP were found in the literature. On the other hand, it is well known that the annealing of implanted A_3B_5 compound semiconductors preferably results in the formation of stacking fault tetrahedra and faulted loops (see, e.g., Ref. 14 and references therein) as well as microtwins. By comparing the ⟨111⟩ stacking sequence of sphalerite InP (InP_{sp}), ...ABCABCABC..., to the ⟨0001⟩ stacking sequence of the wurtzite InP (InP_w), ...ABABABAB..., it can be assumed that the wurtzite InP is a result of the introduction of intrinsic stacking faults (or very thin lamellae of first-order twins) on every third {111} layer of the sphalerite InP. In this approach the process of $InP_{sp} \rightarrow InP_w$ transformation may be activated by shear stress via the generation of Shockley partial dislocations.[9]

In the present work, however, the wurtzite phase of InP appeared as a result of ion-beam-induced (or electron-beam induced) recrystallization of the amorphous surface layer. The surface AL is produced during overlapping of the amorphous cores of the individual latent tracks.[4] According to the model proposed in Ref. 4, the latent amorphous tracks are formed during the very rapid solidification (quenching) of the molten tubes in a single-crystalline matrix, containing the structure defects. There are several consequences of such an amorphization model. First, the process of the track formation is accompanied by shear stress generation in the surrounding matrix. This results in formation of stacking faults, microtwins, and, probably, very small (~2–3 nm) particles of hexagonal structure type, as it is revealed by high-resolution TEM investigations.[15] Second, the track overlapping produces the continuous amorphous layer. However, due to the statistical nature of implantation, inclusions of crystalline InP may still be embedded in the AL even after high dose implantation [see Fig. 1(a)]. Such inclusions may act as nuclei of a crystalline phase growing by ion-beam-induced recrystallization. If the nuclei are faulted or twinned particles, the resulting crystalline phase may inherit a great share of hexagonality.

IV. SUMMARY

In conclusion, the formation of amorphous InP of two different atomic structures is registered after swift Xe-ion irradiation as a consequence of electronic and nuclear energy deposition. An increase of the implantation dose results in partial recrystallization of the amorphous surface layer to polycrystalline InP. The process of recrystallization passes a stage of wurtzite InP phase formation.

ACKNOWLEDGMENTS

This work was supported by the Research Foundation of the Belarusian Academy of Science (Grant No. F97-003). The authors are grateful to S. Klaumünzer and P. Meier, Hahn-Meitner-Institut Berlin, for their assistance during the ion irradiations.

*Author to whom correspondence should be addressed. Present address: Belarusian State University, Kurchatova 7,220064, Minsk, Belarus. Electronic address: gaiduk@rfe.bsu.unibel.by

[1] M. Toulemonde, E. Paumier, and C. Dufour, Radiat. Eff. Defects Solids **126**, 201 (1993).

[2] S. Furuno, H. Otsu, K. Hojou and K. Izui, Nucl. Instrum. Methods Phys. Res. B **107**, 223 (1996).

[3] F. F. Komarov, Langmuir **12**, 199 (1996).

[4] O. Herre, W. Wesch, E. Wendler, P. I. Gaiduk, F. F. Komarov, S. Klaumünzer, and P. Meier, Phys. Rev. B **58**, 4832 (1998); W. Wesch, O. Herre, P. I. Gaiduk, E. Wendler, S. Klaumünzer, and P. Meier, Nucl. Instrum. Methods Phys. Res. B **146**, 341 (1998).

[5] Landolt-Bornstein, *Zahlenwerte und Funktionen aus Physik-Chemie-Astronomie-Geophysik und Technik. 4. teil. Kristalle*. (Springer-Verlag, Berlin, 1955).

[6] D. B. Dove, *in Physics of Thin Films*, edited by G. Hass, M. F. Francombe, and R. W. Hoffman (Academic, New York, 1973).

[7] H. Hirai, Y. Tabira, K. Kondo, T. Oikawa, and N. Ishizava, Phys. Rev. B **52**, 6162 (1995).

[8] V. G. Eremenko and V. I. Nikitenko, Phys. Status Solidi A **14**, 317 (1972).

[9] T. Y. Tan, H. Foll, and S. Hu, Philos. Mag. A **44**, 127 (1981).

[10] Y. K. Vohra, K. E. Brister, S. Desgreniers, A. L. Ruoff, K. J. Chang, and M. L. Cohen, Phys. Rev. Lett. **56**, 1944 (1986).

[11] M. Servidori, S. Campisano, G. Ferla, A. La Ferla, S. U. Compisano, and E. Rimini, Nucl. Instrum. Methods Phys. Res. B **19/20**, 317 (1987).

[12] F. F. Komarov, A. P. Novikov, T. T. Samoiluk, V. S. Solov'yev, and S. Yu. Shiryaev, Radiat. Eff. **90**, 307 (1985).

[13] C. S. Meloni and I. L. Spain, Phys. Rev. B **35**, 7520 (1987).

[14] C. Frigeri, A. Carnera, and A. Gasparotto, Appl. Phys. A: Mater. Sci. Process. **62**, 65 (1996).

[15] P. I. Gaiduk, F. F. Komarov, and W. Wesch, Nucl. Instrum. Methods Phys. Res. B (to be published).